NUCL SCI TECH (2018) 29:137
https://doi.org/10.1007/s41365-018-0474-1

Investigation of production of medical ^{82}Sr and ^{68}Ge for ^{82}Sr/^{82}Rb and ^{68}Ge/^{68}Ga generators via proton accelerator

Ozan Artun[1]

Received: 23 December 2017 / Revised: 24 March 2018 / Accepted: 8 April 2018 / Published online: 28 August 2018

Abstract How to operate ^{82}Sr/^{82}Rb and ^{68}Ge/^{68}Ga generators used in the positron emission tomography scan process is explained, and the importance of ^{82}Sr and ^{68}Ge radionuclides for these generators is revealed. To produce medical ^{82}Sr and ^{68}Ge by means of a proton accelerator in an irradiation time of 24 h, a proton beam current of 250 μA, and an energy range E_{proton} = 100 → 5 MeV, the cross sections and the neutron emission spectrum curves of (p,*x*n) reaction processes on Rb-85, Ga-69 and Ga-71 targets were calculated, and the activities and yields of the product were simulated for the reaction processes. Additionally, the integral yields of the reaction processes were determined via the calculated cross-sectional curves and the mass stopping power obtained from the X-PMSP program. Furthermore, based on the obtained results, the appropriate reaction processes for the production of ^{82}Sr and ^{68}Ge isotopes on Rb-85, Ga-69, and Ga-71 targets are discussed.

Keywords Radioisotope production · Proton accelerator · PET · Radioisotope generators

1 Introduction

Particle accelerators are important because of their applications in different fields, such as radioisotope production in cancer treatment and nuclear battery technology for spacecraft, space probes, and microelectronics [1]. Moreover, for decades, to produce medical radioisotopes used in positron emission tomography (PET), the Los Alamos Neutron Science Center (LANSCE) has produced the medical radioisotopes Sr-82 and Ge-68 for use in PET and the Ac-225 alpha-emitting isotope for use in radioimmunotherapy by means of available linear accelerators (LINACs) with 800-MeV, 200-MeV, and 100-MeV proton beams [2, 3]. Additionally, photonuclear reactions induced by a laser-Compton light source, e.g., the Extreme Light Infrastructure—Nuclear Physics (ELI-NP), which can be used to produce several isotopes of medical interest, have also been addressed recently [4, 5].

The production of radioisotopes Sr-82 and Ge-68 is important because of its use in strontium-82/rubidium-82 and germanium-68/gallium-68 generators. In fact, for clinical imaging, two generators are widely used in PET and the major challenge is that the rubidium-82 and gallium-68 radioisotopes have a short half-life to diagnose diseases and calibrate the PET scanner ($T_{1/2}$ = 75 s and $T_{1/2}$ = 68 min, respectively). However, these isotopes, rubidium-82 and gallium-68, include parent isotopes with longer half-lives, such as strontium-82 ($T_{1/2}$ = 25.5 day) and germanium-68 ($T_{1/2}$ = 271 day), which have been used in cardiac imaging for diagnosing blood flow and in the calibration of PET scanners, respectively [2, 3].

When considering using the daughter radioisotope (i.e., rubidium-82) in PET, the parent isotope, strontium-82, inside generators including an ion exchange column decays to form rubidium-82, and thus, suitable quantities of rubidium-82 together with a certain solution are obtained by pumping via a generator for the PET scan. To illustrate the behavior in the PET scan, a process can be clearly given by [2, 3]:

✉ Ozan Artun
ozanartun@beun.edu.tr; ozanartun@yahoo.com

[1] Department of Physics, Bülent Ecevit University, 67100 Zonguldak, Turkey

(i) $p + {}^{85}Rb \rightarrow {}^{82}Sr + 4n$ (production of Sr-82 on Rb-85 target via (p,4n) reaction)
(ii) ${}^{82}Sr + e^- \rightarrow {}^{82}Rb + \nu$ (production of Rb-82 via electron capture)
(iii) ${}^{82}Rb \rightarrow {}^{82}Kr + e^+ + \nu$ (disintegration to harmless krypton gas in PET scan process)
(iv) $e^+ + e^- \rightarrow 2\gamma$ (gamma rays detectable through detector in positron annihilation event).

The purpose of this study is to estimate productions of parent isotopes Sr-82 and Ge-68 used in ${}^{82}Sr/{}^{82}Rb$ and ${}^{68}Ge/{}^{68}Ga$ generators. The cross sections and the neutron emission spectrum of (p,*x*n) reactions on ${}^{69,71}Ga$ and ${}^{85}Rb$ targets were calculated, and the activities, yield of productions, and integral yields of Sr-82 and Ge-68 in a proton beam current of 250 μA and proton energy of as much as 100 MeV were simulated. Based on the simulated and calculated data, the energy ranges of (p,*x*n) reaction processes for the formations of Sr-82 and Ge-68 in a proton accelerator with 100 MeV are discussed.

2 Calculation and simulation

For an accurate determination of the calculations of nuclear reaction processes of the medical radioisotopes Sr-82 and Ge-68 used in PET for ${}^{82}Sr/{}^{82}Rb$ and ${}^{68}Ge/{}^{68}Ga$ generators, the Talys 1.8 code [6] and *x*-particle mass stopping power (X-PMSP) program [7–9] were used for calculating the cross section of reactions and the mass stopping power of target materials. Talys plays a significant role in the field including nuclear reaction because it includes many nuclear reaction models: equilibrium and pre-equilibrium reaction models, optical model, direct model, compound model, and so on, for low and high energies. For each nuclear model, the Talys code has many calculation applications, such as cross sections, double-differential cross sections, level densities, and emission spectra. The Talys code was used in cross sections and neutron emission spectrum calculations of (p,*x*n) reactions on Rb-85, Ga-68, and Ga-71 targets in the energy range of 1–100 MeV. The calculations of reaction cross sections were performed by using the Fermi gas with constant temperature model for the best input parameters [6–8, 10].

In terms of activity, for the produced nuclei *x*, activity via nuclear reaction on target isotope Y can be expressed by the production rate of nuclei *x*, the decay rate of *x* $\left(\lambda_x = \ln 2/T_x^{1/2}\right)$, and the irradiation time $T_{\text{irradiation}}$:

$$A_x(t) = \lambda_x N_T(0) R_{Y\rightarrow x} T_{\text{irradiation}}. \quad (1)$$

In Eq. (1), $N_T(0)$ is the number of mono-isotopic targets *T* at the start of the irradiation ($t = 0$), $R_{Y\rightarrow x}$ is expressed by the beam current (I_{beam}), the active target volume (V_{target}), and the electron charge

$$R_{Y\rightarrow x} = \frac{I_{\text{beam}}}{z_p q_e} \frac{1}{V_{\text{target}}} \int_{E_{\text{back}}}^{E_{\text{beam}}} \left(\frac{dE}{dx}\right)^{-1} \sigma_x^{\text{rp}}(E) dE, \quad (2)$$

where σ_x^{rp} is the residual production cross section of *x* and z_p represents the projectile charge number [6, 8].

Also, V_{target} can be given by the effective target thicknesses

$$V_{\text{target}} = S_{\text{beam}} \int_{E_{\text{back}}}^{E_{\text{beam}}} \left(\frac{dE}{dx}\right)^{-1} dE, \quad (3)$$

where S_{beam} is the product of the beam surface [6].

In addition to the Talys code, another program, X-PMSP, was used to determine the integral yields of reaction processes from reaction cross sections and the mass stopping powers of target materials. It can calculate the mass stopping powers and ranges of 98 elements for proton, deuteron, triton, he-3, and alpha particles in the energy range between 1 and 1000 MeV.

The mass stopping powers of Rb-85, Ga-68, and Ga-71 targets for protons can be calculated by means of the velocity of the incident particle $\beta(v/c)$, as follows:

$$\left(\frac{dE}{\rho dx}\right) = 0.3071 \frac{Zz^2}{A\beta^2} \left[13.8373 + \ln\left(\frac{\beta^2}{1-\beta^2}\right) - \beta^2 - \ln(I) - \frac{\delta}{2}\right], \quad (4)$$

where *A* and *Z* are the mass and the proton number of the target, respectively, and *z* and *I* denote the atomic number of the incident particle and the mean ionization potential of the target material, respectively. The density effect correction (δ) for different X $\left(\log\left(\beta/\sqrt{1-\beta^2}\right)\right)$ values is given by

$$\begin{aligned} &\text{(i) } \delta(X) = 4.6052X + a(X_1 - X)^m + C (X_0 < X < X_1) \\ &\text{(ii) } \delta(X) = 4.6052X + C \quad (X > X_1), \\ &\text{(iii) } \delta(X) = \delta(X_0) \times 10^{2(X-X_0)} \quad (X \le X_0), \end{aligned} \quad (5)$$

where a, X_1, X_0, and C are the constants of the medium [7].

However, the integral yields of the reaction processes for the irradiation time *t* and the projectile current *I* can be calculated by the reaction cross section ($\sigma(E)$) and the mass stopping power $\left(\frac{dE}{d(\rho x)}\right)$ in (MeVcm^2/g) for the activation equation:

$$A = \frac{N_A H}{M} I\left(1 - e^{-\lambda t}\right) \int_{E_1}^{E_2} \frac{\sigma(E) dE}{\left(\frac{dE}{d(\rho x)}\right)}, \quad (6)$$

where λ and *H* are the decay constant of product and isotopic abundance of target nuclei, respectively. *M* represents

the atomic weight of target material, and N_A is Avogadro's number [8].

2.1 Material and methodology

In the current work, to produce parent isotopes Sr-82 and Ge-68 of daughter isotopes Rb-82 and Ga-68 for ^{82}Sr/^{82}Rb and ^{68}Ge/^{68}Ga generators on Rb-85, Ga-68, and Ga-71 targets, simulations of the reaction processes under particular conditions were performed to define activity and yield results for (p,*x*n) reactions in the energy range E_{proton} = 100 → 5 MeV. Ga-68, Ga-71, and Rb-85 targets were assumed to have > 99% purity and uniform thickness, and density in reaction processes. During the (p,*x*n) reaction processes, it was assumed that there were no losses in the yield and activity of the reactions. The effective target thicknesses of Rb-85, Ga-71, and Ga-69 were 8.270 cm, 2.076 cm, and 2.017 cm in the energy range E_{proton} = 100 → 5 MeV, respectively. Considering the proton energy range and beam current of the accelerator made it possible to adjust the most suitable target thicknesses by code. The densities of the target materials were 1.530 g/cm^3 (for Rb-85) and 5.910 g/cm^3 (for Ga-71 and Ga-69), and the area of all target materials was approximately 1.00 cm^2. Moreover, to irradiate the target materials, a proton accelerator with a proton beam current of 250 μA in the energy range E_{proton} = 100 → 5 MeV was used, and the irradiation time of the target materials Rb-85, Ga-71, and Ga-69 for all reaction processes was 24 h and the cooling time of the target materials was 24 h. The maximum produced heat in the targets for the production of Sr-82 and Ge-68 was approximately 23.750 kW. Under these conditions, the yields of product and activities in proton-induced reactions on Rb-85, Ga-71, and Ga-69 targets were simulated for 24 different reactions, including ^{85}Rb(p,4n)^{82}Sr, ^{71}Ga(p,4n)^{68}Ge, and ^{69}Ga(p,2n)^{68}Ge [2, 3, 6].

3 Results and discussion

To assess the importance of the production of Sr-82 and Ge-68 used in ^{82}Sr/^{82}Rb and ^{68}Ge/^{68}Ga generators, the cross sections of 24 different (p,*x*n) reactions on Rb-85, Ga-71, and Ga-69 target materials were calculated. The proton energies with the maximum cross sections of reactions were also determined. Based on the obtained energy values, the neutron emission spectrum results of reactions were calculated, and the neutron emission energies of reactions were estimated. Moreover, the activities and yields of product of the reactions were simulated under particular conditions using a proton accelerator in the energy range E_{proton} = 100 → 5 MeV. Additionally, the integral yields of reactions were determined by the obtained cross sections and the mass stopping powers of the targets. On the basis of our results, we discussed suitable productions of Sr-82 and Ge-68 in (p,*x*n) reaction processes.

3.1 Calculation of cross section

In the description of the production parent isotopes Sr-82 and Ge-68 used in ^{82}Sr/^{82}Rb and ^{68}Ge/^{68}Ga generators, the cross sections for 24 different reactions on Rb-85, Ga-71, and Ga-69 target materials were calculated in the 1–100-MeV energy range, and the results are presented in Figs. 1, 2 and 3. For the medical radioisotope Sr-82 on the Rb-85 target, the calculated cross-sectional curves and the experimental data in the literature are shown in Fig. 1, which illustrates nine reactions. As is clearly visible in Fig. 1, ^{85}Rb(p,n)^{85}Sr, ^{85}Rb(p,4n)^{82}Sr, ^{85}Rb(p,3n)^{83}Sr, and ^{85}Rb(p,5n)^{81}Sr reactions include few experimental results, and the calculated cross-sectional result for ^{85}Rb(p,n)^{85}Sr reaction is in good agreement with the findings of Kiss et al. [11] and Levkovski [12]. In the ^{85}Rb(p,3n)^{83}Sr reaction, the theoretical cross-sectional result is more consistent with the results of Levkovski [12] than the data reported by Kastleiner et al. [13]. Although the theoretical cross-sectional curve of the ^{85}Rb(p,4n)^{82}Sr reaction is similar to the result of Kastleiner et al. [13], the maximum cross-sectional values of both results are approximately 45 MeV, but the experimental cross-sectional result of Horiguchi et al. [14] has a maximum cross-sectional value at an ∼ 50 MeV incident proton energy. In the ^{85}Rb(p,5n)^{81}Sr reaction, the theoretical cross-sectional results and the experimental cross-sectional results [14, 13] are fairly low, and the maximum cross-sectional value is ∼ 58 MeV. The cross-sectional results for (p,*x*)^{86}Sr, (p,6n)^{80}Sr, (p,7n)^{79}Sr, and (p,8n)^{80}Sr reactions reach values that are too low compared with other reactions.

As can be observed, (p,n), (p,2n), (p,3n), (p,4n), and (p,5n) reactions have cross-sectional curves; in particular, the ^{85}Rb(p,2n)^{84}Sr reaction has the highest cross-sectional values at 19 MeV, and the cross-sectional curve of this reaction is intersected by ^{85}Rb(p,n)^{85}Sr and ^{85}Rb (p,3n)^{83}Sr at 14 MeV and 27 MeV proton incident energies, respectively. ^{85}Rb(p,n)^{85}Sr and ^{85}Rb(p,3n)^{83}Sr reactions in ^{85}Rb(p,*x*n) reactions create contamination for the production of Sr-84. Similarly, the ^{85}Rb(p,3n)^{83}Sr reaction is intersected by ^{85}Rb(p,2n)^{84}Sr and ^{85}Rb(p,4n)^{82}Sr at 27 MeV and 43 MeV proton incident energies, respectively. In the case of the ^{85}Rb(p,4n)^{82}Sr reaction, the cross-sectional curve of this reaction is cut by ^{85}Rb(p,3n)^{83}Sr behind 43 MeV. However, the cross-sectional values for the ^{85}Rb(p,5n)^{81}Sr reaction are not enough to cut off ^{85}Rb(p,4n)^{82}Sr reaction.

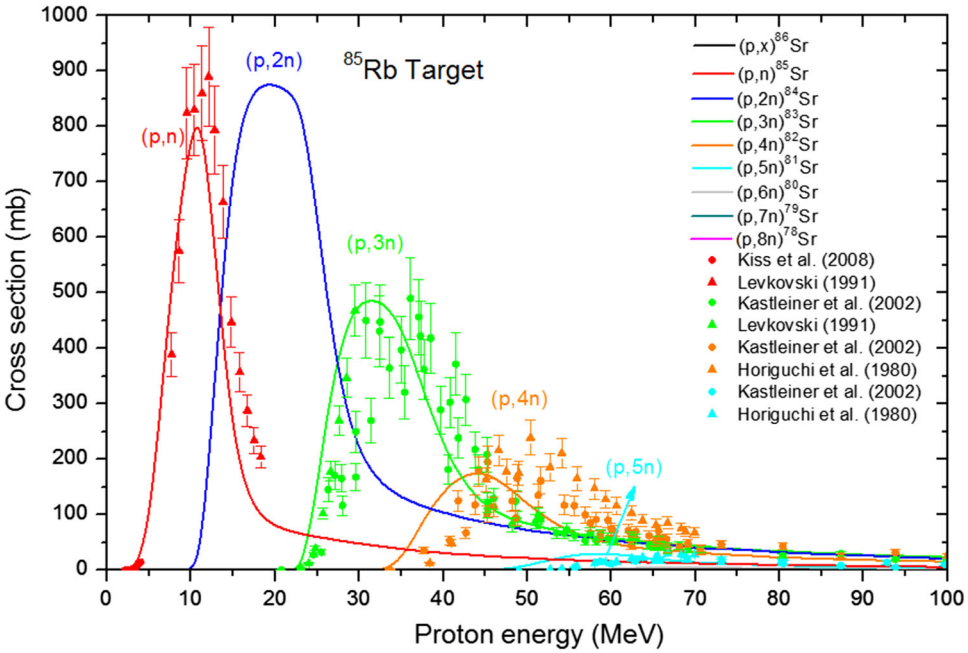

Fig. 1 (Color online) Calculated cross sections of (p,*x*n) reaction processes on Rb-85 target

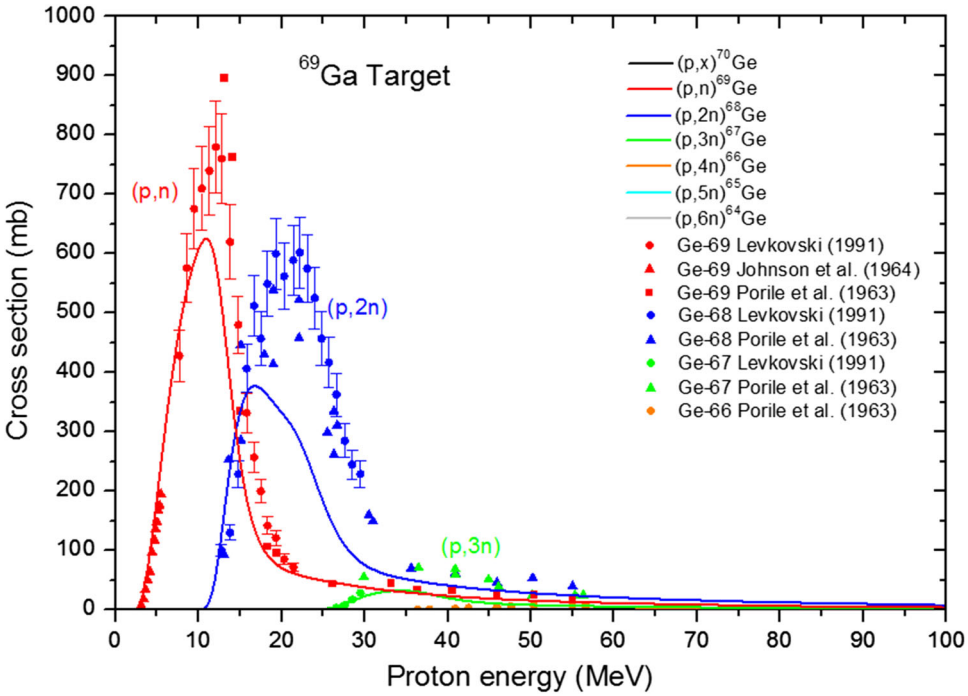

Fig. 2 (Color online) Calculated cross sections of (p,*x*n) reaction processes on Ga-69 target

The calculated cross-sectional curves and the experimental results of Levkovski [12] and Porile et al. [15] for (p,*x*n) reactions on the Ga-69 target are shown in Fig. 2. To produce the radionuclide Ge-68, the ^{69}Ga(p,2n)^{68}Ge reaction process has two experimental results, as reported by Levkovski [12] and Porile et al. [15]. The calculated result agrees well with both the experimental data from threshold energy to 17 MeV; the cross-sectional values of these two experimental results, however, are higher than the calculated results. For the ^{69}Ga(p,n)^{69}Ge reaction, three experimental data together with the results of Levkovski [12] and Porile et al. [15] are available, and the experimental result of Johnson et al. [16] is in good agreement with the theoretical cross-sectional curves in the energy range between 3 and 6 MeV. In the production of Ge-68, beyond 25 MeV, ^{69}Ga(p,n)^{69}Ge and ^{69}Ga(p,3n)^{67}Ge reactions make up contamination in the ^{69}Ga(p,2n)^{68}Ge reaction. The cross-sectional result of ^{69}Ga(p,3n)^{67}Ge is lower

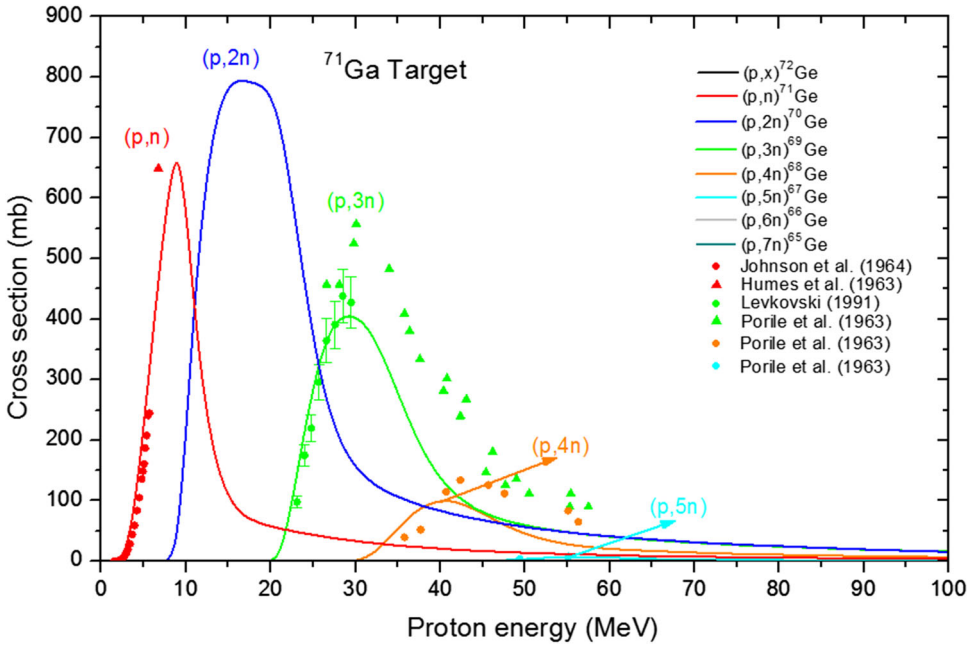

Fig. 3 (Color online) Calculated cross sections of (p,*x*n) reaction processes on Ga-71 target

than the (p,n) and (p,2n) reactions on the Ga-69 target. Because the ^{69}Ga(p,*x*)^{70}Ge, ^{69}Ga(p,4n)^{66}Ge, ^{69}Ga(p,5n)^{65}Ge, and ^{69}Ga(p,6n)^{64}Ge reactions have cross-sectional values that are too low, these reactions do not affect the production of the ^{69}Ga(p,2n)^{68}Ge reaction in terms of contamination.

For an accurate determination of the production of nuclei, the comparisons of the theoretical cross section and the experimental data by Levkovski [12], Porile et al. [15], Johnson et al. [16], and Humes et al. [17] for (p,*x*n) on Ga-71 target material are shown in Fig. 3. For the ^{71}Ga(p,n)^{71}Ge reaction, there are two experimental data by Johnson et al. [16] and Humes et al. [17]. The calculated cross-sectional result of this reaction is in considerably good agreement with the results of Johnson et al. [16], but Humes et al. [17] have only one data point at 5 MeV that is different from the theoretical result. Unfortunately, there are no experimental measurements of the ^{71}Ga(p,2n)^{70}Ge reaction in the literature. The calculated cross-sectional result of the ^{71}Ga(p,3n)^{69}Ge reaction agrees with Levkovski's [12] data, and the maximum cross section for this reaction is at ~ 29 MeV incident proton energy. In the case of the most important reaction, it is clear that ^{71}Ga(p,4n)^{68}Ge has low cross-sectional curves compared with (p,n), (p,2n), and (p,3n), and the cross-sectional curves of these three reactions cut ^{71}Ga(p,4n)^{68}Ge at ~ 33 MeV, ~ 38 MeV, and ~ 45 MeV proton incident energies.

3.2 Calculation of differential cross section of (p,*x*n) reactions

Here, the determination of the cross section of the (p,*x*n) reactions is quite important to estimate the incident proton energy values; hence, the incident proton energies corresponding to the maximum cross section for suitable (p,*x*n) reactions were determined by cross-sectional calculations, as shown in Figs. 1, 2 and 3. The differential cross-sectional (DX) calculations for (p,*x*n) reactions on Rb-85, Ga-69, and Ga-71 targets are presented in Fig. 4a–c. For the Rb-85 target, the calculated DX results of the ^{85}Rb(p,n)^{85}Sr, ^{85}Rb(p,2n)^{84}Sr, ^{85}Rb(p,3n)^{83}Sr, ^{85}Rb(p,4n)^{82}Sr, and ^{85}Rb(p,5n)^{81}Sr reactions are given by Fig. 4a as a function of neutron energy. DXs of these reactions have evaporation peaks in the energy range between 0.5 and 1.5 MeV. Except for ^{85}Rb(p,n)^{85}Sr, the DX values of the other reactions reach as much as 1000 mb/MeV. Similarly, in Fig. 4b, c, the calculated DX results on Ga-69 and Ga-71 targets reach the maximum values for all reactions in the energy range 0.5-1.0 MeV. This clearly indicates that the DX values of ^{85}Rb(p,4n)^{82}Sr, ^{69}Ga(p,2n)^{68}Ge, and ^{71}Ga(p,4n)^{68}Ge reactions in the production of Sr-82 and Ge-68 are 975.54 mb/MeV at ~ 0.94 MeV neutron emission energy, 455.72 mb/MeV at ~ 0.59 MeV, and 743.77 mb/MeV at ~ 0.85 MeV.

3.3 Simulation of activity and yield of product

To analyze (p,*x*n) reactions on Rb-85, Ga-69, and Ga-71 targets in E_{proton} = 100 → 5 MeV, 24 h irradiation time, and proton beam current of 250 μA by means of a proton

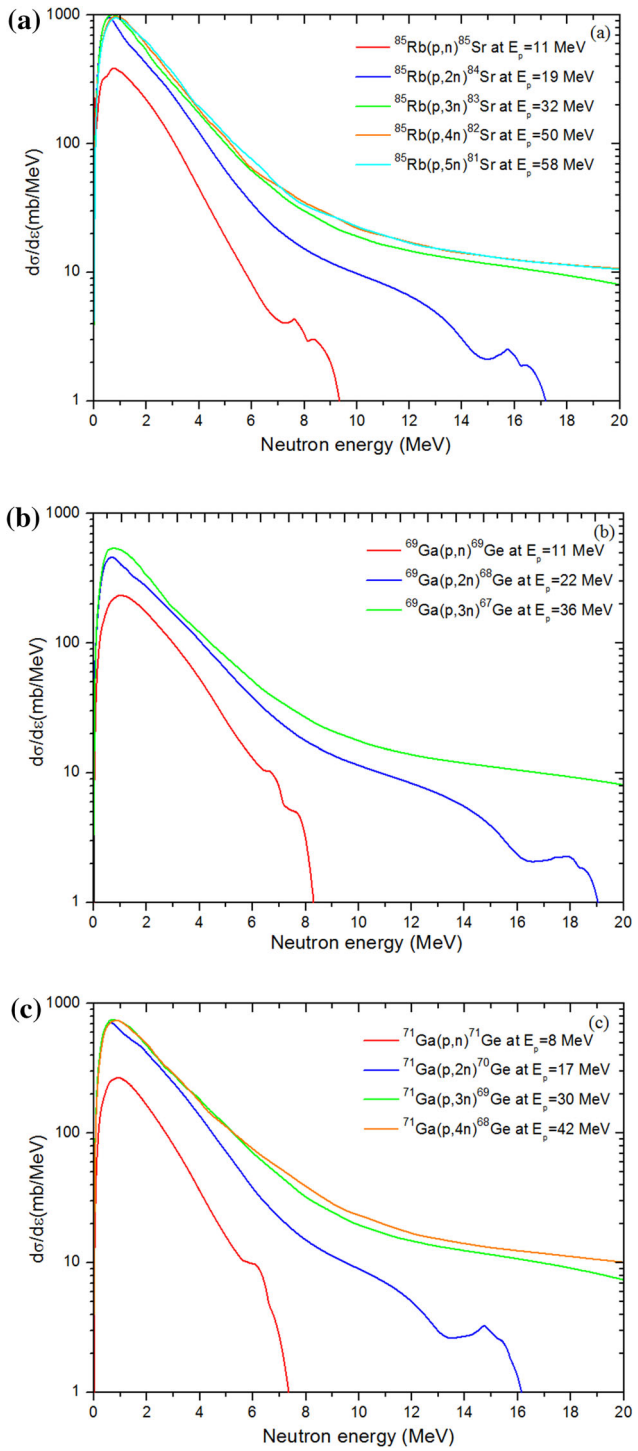

Fig. 4 (Color online) DX calculations of suitable reaction processes for Rb-85 (**a**), Ga-69 (**b**), and Ga-71 (**c**) targets

accelerator, the simulated activities and yield of products for 24 different (p,*x*n) reactions under certain conditions were considered, and the simulations are shown in Figs. 5, 6 and 7. In the simulations, there are nine (p,*x*n) reactions on the Rb-85 target, and among these reactions, the highest activities are (p,3n)^{83}Sr (∼ 4800 MBq) and (p,5n)^{81}Sr (∼ 1265 MBq) at the end of 24 h. (p,2n)^{83}Sr and (p,*x*)^{86}Sr reactions have no activity values, because ^{83}Sr and ^{86}Sr are natural isotopes of Sr. (p,7n)^{79}Sr and (p,8n)^{78}Sr reactions have constant activities during the irradiation time, because the half-lives of ^{79}Sr and ^{78}Sr isotopes ($T_{1/2}$ = 2.25 min and $T_{1/2}$ = 2.65 min) are short compared with the irradiation time (hour); therefore, the activities of these two isotopes seem to be straight lines. A similar situation is observed for ^{65}Ge and ^{64}Ge ($T_{1/2}$ = 30.9 s and $T_{1/2}$ = 63.7 s). The activity value of (p,4n)^{82}Sr increases with increasing irradiation time, and its activity reaches ∼ 157.81 MBq in 24 h of irradiation time. In the case of (p,*x*n) reactions on Ga-69 and Ga-71 target materials, the (p,3n) reaction has a high activity compared with other reactions for both targets, except for the (p,n)^{69}Ge reaction with an irradiation time of more than 15 h. Because Ge-70 and Ge-72 are stable isotopes of Ge, there are no activities, as shown in Figs. 6 and 7. Additionally, the activity of the ^{69}Ga(p,n)^{69}Ge reaction has the highest values in 24 h (∼ 1698.9 MBq); furthermore, the production of ^{69}Ge for the Ga-71 target with the (p,3n) reaction also has the highest activity (∼ 3716.7 MBq). For the Ge-68 radionuclide used in PET, the activities of ^{69}Ga(p,2n)^{68}Ge and ^{71}Ga(p,4n)^{68}Ge reactions are ∼ 16.63 MBq and ∼ 9.03 MBq in 24 h.

However, the yields of product of (p,*x*n) reactions on Rb-85, Ga-69, and Ga-71 targets as a function of irradiation time under the conditions mentioned in the activity simulations were simulated and are shown in Figs. 8, 9 and 10. In the productions of radionuclides Sr on the Rb-85 target (Fig. 8), there are a few interesting reactions compared with the activities of such reactions as (p,5n)^{81}Sr and (p,6n)^{80}Sr. The (p,5n)^{81}Sr reaction has the highest yield values up to 2 h of irradiation time; however, its yield curve decreases as a sharp curve, reaching zero at 6.2 h. There are similar states for (p,6n)^{80}Sr, (p,7n)^{79}Sr, and (p,8n)^{78}Sr. This is mainly because ^{80}Sr, ^{79}Sr, and ^{78}Sr isotopes produced by ^{85}Rb(p,6n), ^{85}Rb(p,7n), and ^{85}Rb(p,8n) reactions have half-lives of 106.3 min, 2.25 min, and 2.65 min, respectively; thus, these radioisotopes disappear up to a few hours because of decay. In other words, the productions of ^{79}Sr and ^{78}Sr isotopes are performed by ^{85}Rb(p,7n) and ^{85}Rb(p,8n) reactions at the highest amount in the first few minutes of irradiation, but at the end of 1 h, the yields of product of ^{79}Sr and ^{78}Sr isotopes are close to zero, because new productions of ^{79}Sr and ^{78}Sr isotopes are not available. This is because the target material has not been changed up to the end of irradiation time ($t_{irradiation} \rightarrow$ 24h). The (p,n)^{85}Sr, (p,3n)^{83}Sr, and (p,4n)^{82}Sr reactions during the irradiation process have almost constant yield values of 9.08 MBq/mA, 617.64 MBq/mA, and 25.95 MBq/mA, respectively. In the production of radionuclides of Ge on Ga-69 and Ga-71 targets, when Figs. 9 and 10 for product of yield are compared with each other, the yields

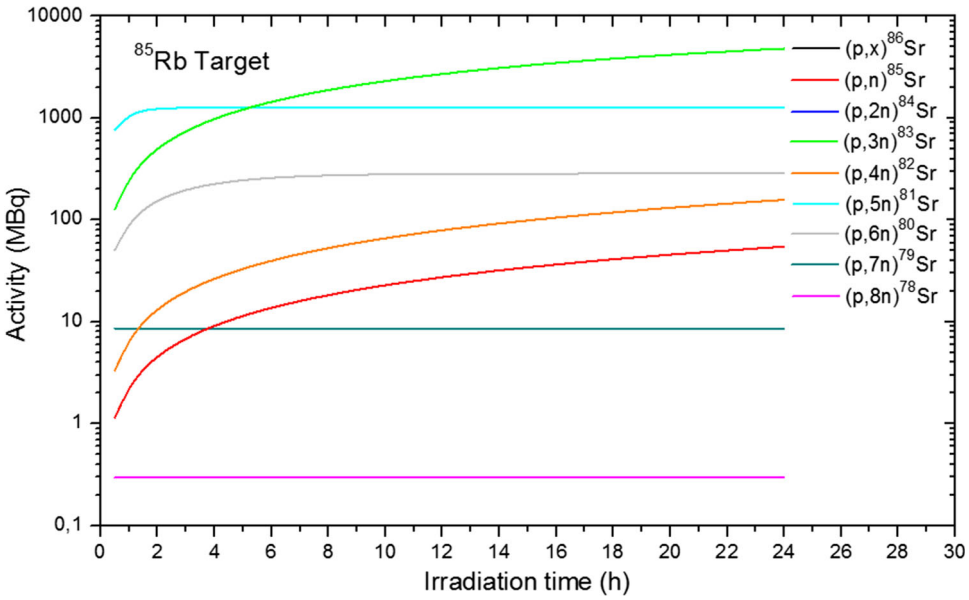

Fig. 5 (Color online) Simulated activities of (p,*x*n) reactions on Rb-85 as a function of irradiation time

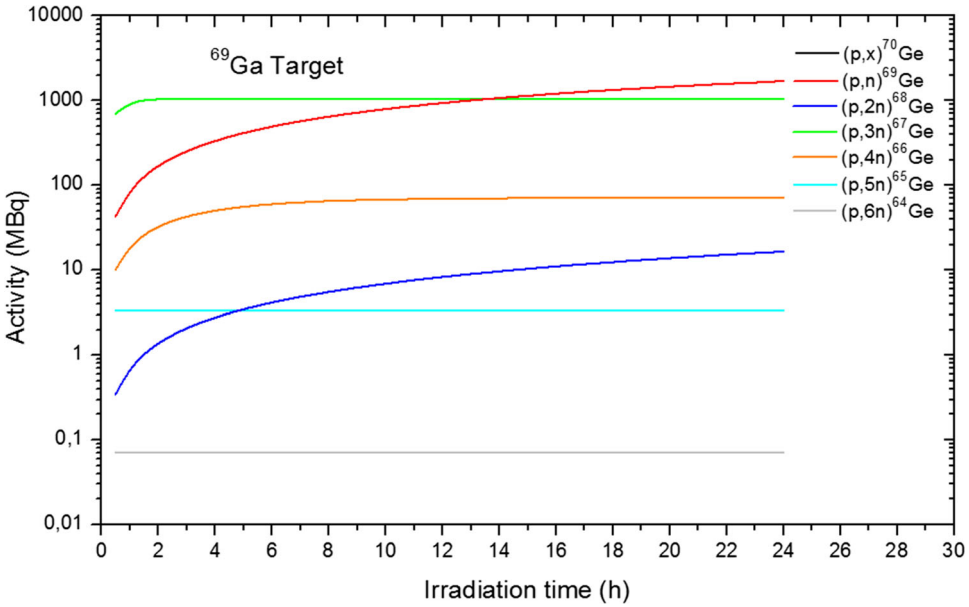

Fig. 6 (Color online) Simulated activities of (p,*x*n) reactions on Ga-69 as a function of irradiation time

of product of Ge-69 have two different values (p,n)^{69}Ge (228.09 MBq/mA) and (p,3n)^{69}Ge (499.04 MBq/mA). The yields of Ge-69 on the Ga-71 target are higher than that of production on Ga-69. In contrast to this reaction, the productions of the radionuclides ^{65,66,67,68}Ge on the Ga-69 target have higher yield values than on the Ga-71 target. Moreover, the ^{69}Ga(p,n)^{69}Ge, ^{69}Ga(p,2n)^{68}Ge, ^{71}Ga(p,3n)^{69}Ge, ^{71}Ga(p,n)^{71}Ge, and ^{71}Ga(p,4n)^{68}Ge reactions have almost constant yield values during irradiation time, i.e., 228.10 MBq/mA, 2.77 MBq/mA, 499.04 MBq/mA, 37.80 MBq/mA, and 1.50 MBq/mA, respectively. However, the yield values of the ^{69}Ga(p,3n)^{67}Ge, ^{69}Ga(p,4n)^{66}Ge, ^{71}Ga(p,5n)^{67}Ge, and ^{71}Ga(p,5n)^{67}Ge reactions approach zero with increasing irradiation time.

3.4 Integral yield calculations for (p,*x*n) reactions

To estimate the integral yields of (p,*x*n) reactions on Rb-85, Ga-69, and Ga-71 targets using Eq. (6), cross-sectional results were used that were obtained from Figs. 1, 2 and 3 and the mass stopping powers of the target materials (Fig. 11) calculated by the X-PMSP program for targets. The integral yield calculations were performed in certain conditions, such as irradiation time of 24 h, proton beam current of 250 μA, and the energy range of 1–100 MeV. Isotopic enrichment of each target material was taken into account in the calculations of integral yield reactions.

The production of Sr isotopes on Rb-85 is shown in Fig. 12a, and the integral yields of (p,n)^{85}Sr, (p,3n)^{83}Sr,

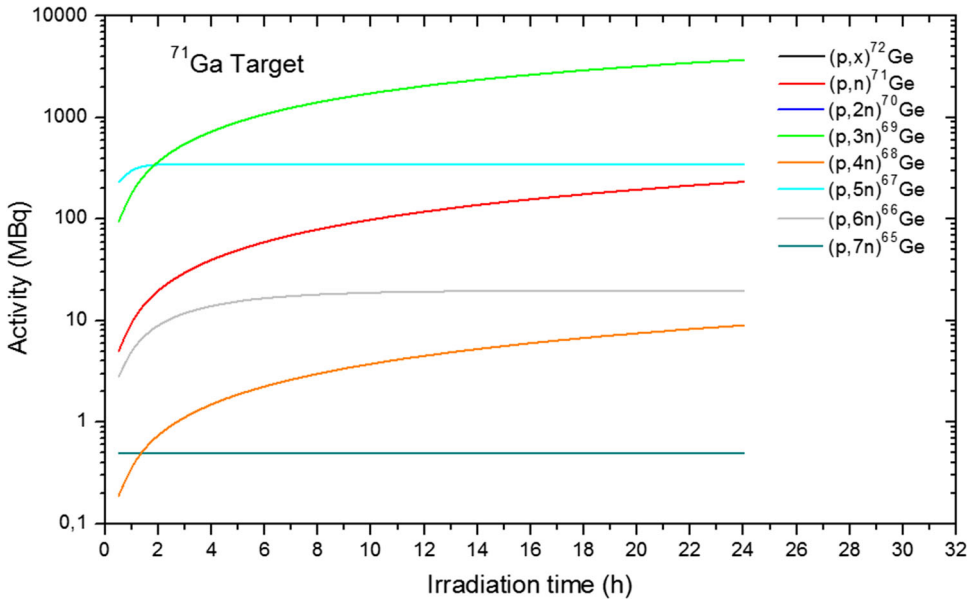

Fig. 7 (Color online) Simulated activities of (p,*x*n) reactions on Ga-71 as a function of irradiation time

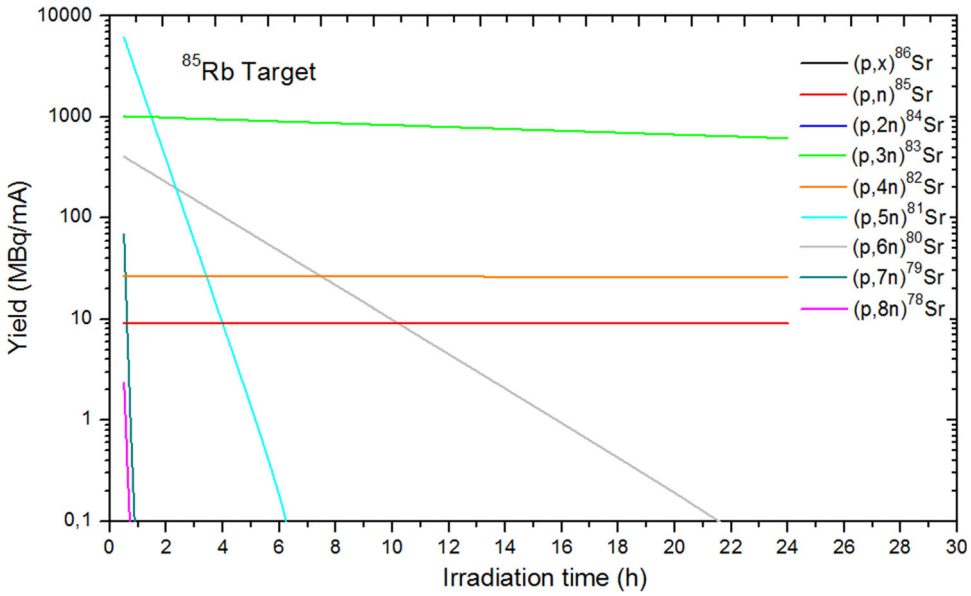

Fig. 8 (Color online) Simulated yields of (p,*x*n) reactions on Rb-85 as a function of irradiation time

(p,4n)^{82}Sr, and (p,5n)^{81}Sr reactions have high values (see Fig. 1) of 150 MBq/μA, 16,000 MBq/μA, 350 MBq/μA, and 4000 MBq/μA at 100 MeV, respectively. Figure 12a, for the production of medical Sr-82, clearly shows that Sr-82 formed approximately 95% up to 60 MeV of proton incident energy; especially, after 40 MeV, the production of Sr-82 steeply increased at this energy, but the production of Sr-85 and Sr-83 in (p,*x*n) reactions was saturated. Then, Sr-81 was involved in these (p,*x*n) reactions beyond 45 MeV. The integral yields of Ge-68 for Ga-71 and Ga-69 targets are shown in Fig. 12b, c.

The integral yield results of ^{69}Ga(p,2n)^{68}Ge and ^{71}Ga(p,4n)^{68}Ge reactions are 40 MBq/μA and 15 MBq/μA, respectively; these results indicate that the integral yield value for the ^{69}Ga(p,2n)^{68}Ge reaction is bigger than that of ^{71}Ga(p,4n)^{68}Ge. Additionally, the production of Ge-68 in the ^{69}Ga(p,2n)^{68}Ge reaction reaches approximately 85% at 30-MeV proton incident energy; the production of Ge-68 in the ^{71}Ga(p,4n)^{68}Ge reaction, however, is saturated at ~ 55 MeV. Furthermore, the production of Ge-68 in the (p,*x*n) process begins at 12 MeV on the ^{69}Ga target, as in Fig. 12b. In contrast, the formation of Ge-68 in (p,4n) on the Ga-71 target begins at 32 MeV, as in Fig. 12c. Therefore, based on integral yield, it can be said that the ^{69}Ga(p,2n)^{68}Ge reaction is more suitable than that of ^{71}Ga(p,4n)^{68}Ge in terms of the incident proton energy and yield values of the reactions. Moreover, in addition to the Ge-69 radionuclide, there is contamination of the

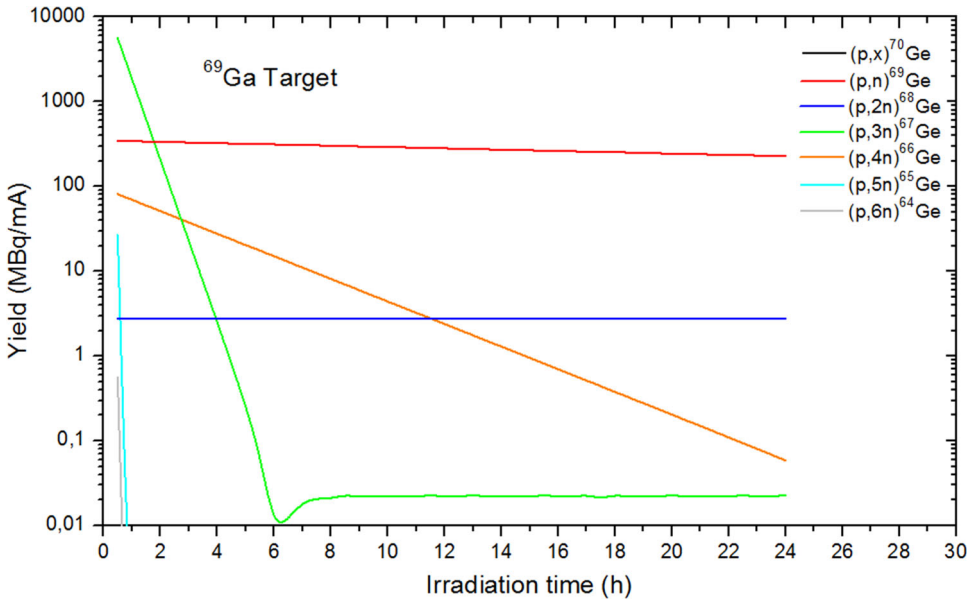

Fig. 9 (Color online) Simulated yields of (p,*x*n) reactions on Ga-69 as a function of irradiation time

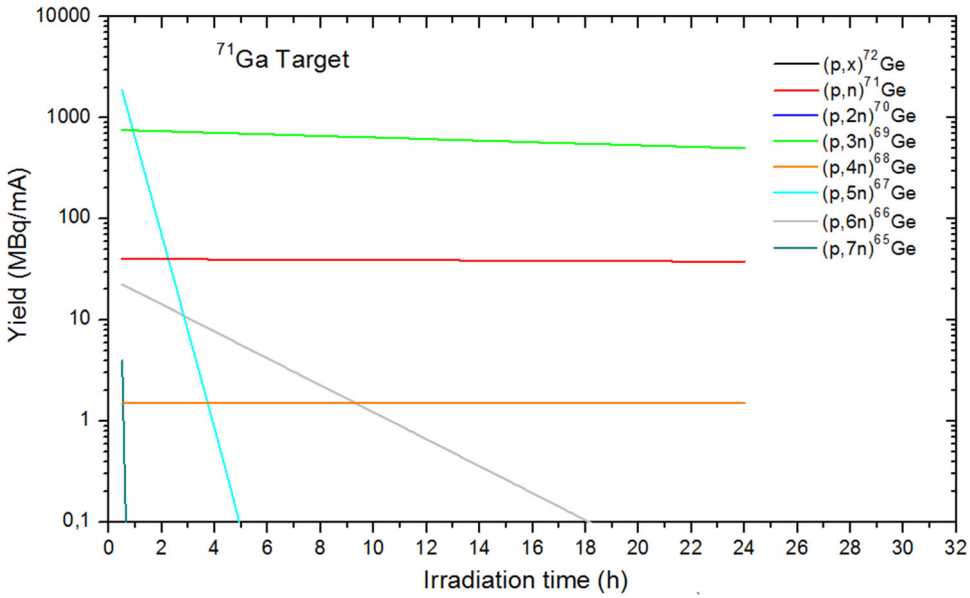

Fig. 10 (Color online) Simulated yields of (p,*x*n) reactions on Ga-71 as a function of irradiation time

^{71}Ga(p,n)^{71}Ge reaction in the production of Ge-68 on the Ga-71 target beyond 3 MeV, as in Fig. 12c, compared with the Ga-69 target.

4 Summary

The cross sections and DXs of (p,*x*n) reaction processes were calculated to produce the radionuclides Sr-82 and Ge-68 used in PET for strontium-82/rubidium-82 and germanium-68/gallium-68 generators by means of a proton accelerator. The activities and yields of the product of (p,*x*n) processes on Rb-85, Ga-69, and Ga-71 targets were simulated under particular conditions, such as under an irradiation time 24 h and a proton beam current of 250 μA. Additionally, the integral yields of these reaction processes were determined by the calculated cross-sectional curves and the mass stopping powers via X-PMSP.

The results obtained from calculations clearly show that the emission spectrum curves for the suitable (p,*x*n) reactions on Rb-85, Ga-68, and Ga-71 targets have the highest values in the energy range between 0.5 and 1.0 MeV. For the productions of Sr-82 and Ge-68, the DX values of the ^{85}Rb(p,4n)^{82}Sr, ^{69}Ga(p,2n)^{68}Ge, and ^{71}Ga(p,4n)^{68}Ge reactions are 975.54 mb/MeV at ∼ 0.94 MeV neutron emission energy, 455.72 mb/MeV at ∼ 0.59 MeV, and 743.77 mb/MeV at ∼ 0.85 MeV. Upon taking the yields of the product into account, the productions of the radionuclides

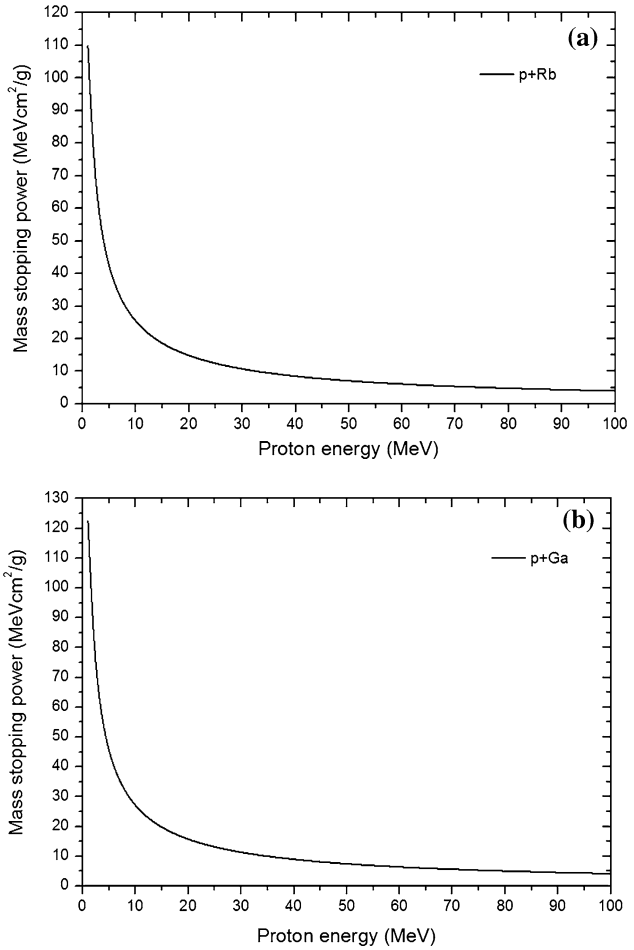

Fig. 11 Mass stopping powers of proton-charged particle for Rb (**a**) and Ga (**b**) targets

^{65,66,67,68}Ge on the Ga-69 target have higher yield values than on the Ga-71 target. Furthermore, as another result, the yield values of the (p,6n)^{80}Sr, (p,7n)^{79}Sr, (p,8n)^{78}Sr, (p,n)^{85}Sr, (p,3n)^{83}Sr, and (p,4n)^{82}Sr reactions up to the end of irradiation are almost constant.

When analyzing the integral yields of (p,*x*n) reaction processes, it is important to note that the integral yield value for the ^{69}Ga(p,n)^{68}Ge reaction is lower than that for ^{71}Ga(p,4n)^{68}Ge. Additionally, the production of Ge-68 in the ^{69}Ga(p,2n)^{68}Ge reaction is saturated by approximately 85% at a 30-MeV proton incident energy. In the case of the ^{71}Ga(p,4n)^{68}Ge reaction, the production of Ge-68 is saturated at $\sim$ 55 MeV. Therefore, the ^{69}Ga(p,2n)^{68}Ge reaction is more suitable than that of ^{71}Ga(p,4n)^{68}Ge in terms of proton incident energy and yield value of reaction. The productions of medical ^{82}Sr and ^{68}Ge for ^{82}Sr/^{82}Rb and ^{68}Ge/^{68}Ga generators can be carried out by a LINAC with 70-MeV proton incident energy and with a high-beam current intensity, such as LANSCE in Los Alamos Laboratory and BLIP in Brookhaven.

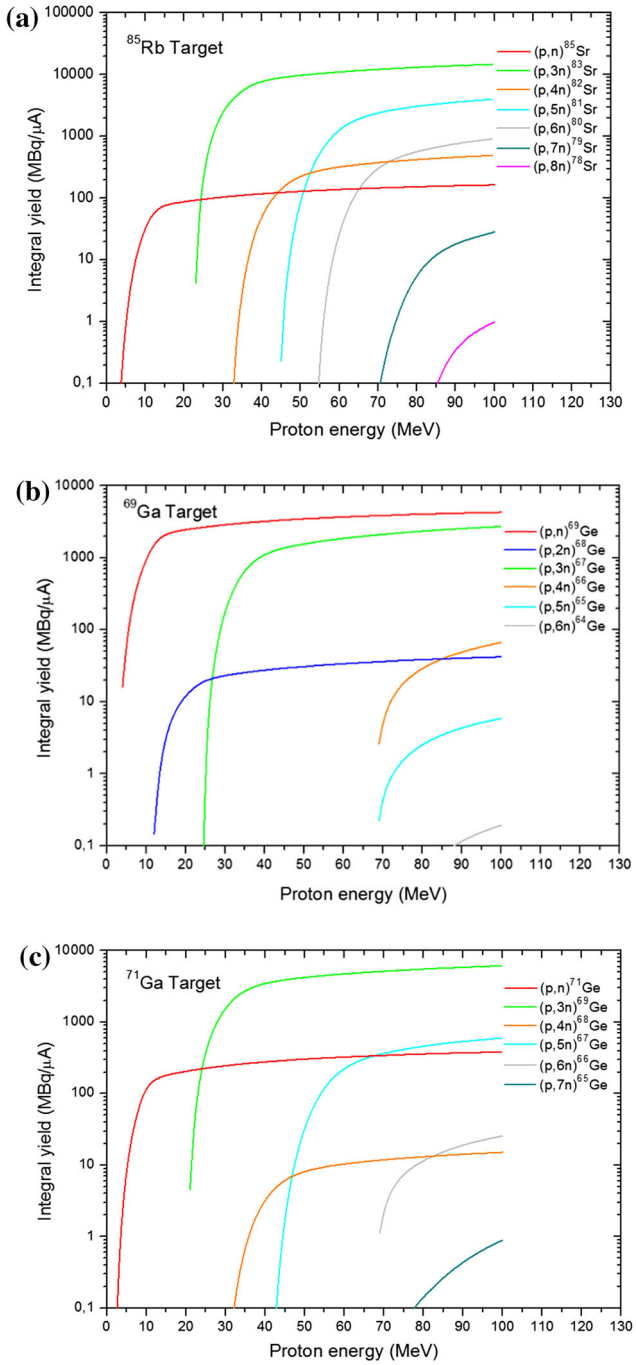

Fig. 12 (Color online) Calculated integral yields of reaction processes for Rb-85 (**a**), Ga-69 (**b**), and Ga-71 (**c**) targets

References

1. O. Artun, A study of nuclear structure for ^{244}Cm, ^{241}Am, ^{238}Pu, ^{210}Po, ^{147}Pm, ^{137}Cs, ^{90}Sr and ^{63}Ni nuclei used in nuclear battery. Mod. Phys. Lett. A **32**, 1750117 (2017). https://doi.org/10.1142/S0217732317501176
2. E.J. Peterson, LANSCE into the future. Los Alamos Sci **30**, 112 (2006)

3. Los Alamos National Laboratory, Accelerator Radioisotopes Save Lives: Part II Actinide Research Quarterly October, 1–40 (2010)
4. W. Luo, Production of medical radioisotope 64Cu by photoneutron reaction using ELI-NP γ-ray beam. Nucl. Sci. Technol. **27**, 96–100 (2016). https://doi.org/10.1007/s41365-016-0094-6
5. W. Luo, M. Bobeica, I. Gheorghe et al., Estimates for production of radioisotopes of medical interest at extreme light infrastructure—nuclear physics facility. Appl. Phys. B **122**, 8–18 (2016). https://doi.org/10.1007/s00340-015-6292-9
6. A. Koning, S. Hilaire, S. Goriely, Talys manual 1.8, (2015) ⟨http://www.talys.eu/fileadmin/talys/user/docs/talys1.8.pdf⟩. Accessed 1 Dec 2017.
7. O. Artun, Estimation of the production of medical Ac-225 on thorium material via proton Accelerator. Appl. Radiat. Isot. **127**, 166–172 (2017). https://doi.org/10.1016/j.apradiso.2017.06.006
8. O. Artun, Investigation of the production of cobalt-60 via particle accelerator. Nuc. Tech. Rad. Protec. **32**(4), 327–333 (2017). https://doi.org/10.2298/NTRP1704000A
9. O. Artun, X-particle mass stopping power code (2017) ⟨https://www.x-pmsp.com/⟩
10. O. Artun, Investigation of the production of promethium-147 via particle accelerator. Indian J. Phys. **91**, 909–914 (2017). https://doi.org/10.1007/s12648-017-0997-z
11. G.G. Kiss, T. Rauscher, G. Gyürky et al., Coulomb suppression of the stellar enhancement factor. Phys. Rev. Lett. **101**, 191101 (2008). https://doi.org/10.1103/PhysRevLett.101.191101
12. V.N. Levkovski, *Cross sections of medium mass nuclide activation(A = 40–100) by medium energy protons and alpha-particles (E = 10–50 MeV, Act. Cs. By protons and alphas* (USSR, Moscow, 1991)
13. S. Kastleiner, S.M. Qaim, F.M. Nortier et al., Excitation functions of ^{85}Rb(p,*x*n)$^{85m,\ g,\ 83,82,81}$Sr reactions up to 100 MeV: integral tests of cross section data, comparison of production routes of ^{83}Sr and thick target yield of ^{82}Sr. Appl. Radiat. Isot. **56**, 685–695 (2002). https://doi.org/10.1016/S0969-8043(01)00267-6
14. T. Horiguchi, H. Noma, Y. Yoshizawa et al., Excitation functions of proton induced nuclear reactions on 85Rb. Appl. Radiat. Isot. **31**, 141–151 (1980). https://doi.org/10.1016/0020-708X(80)90138-6
15. N.T. Porile, S. Tanaka, H. Amano et al., Nuclear reactions of Ga69 and Ga71 with 13–56 MeV protons. Nucl. Phys. **43**, 500–522 (1963). https://doi.org/10.1016/0029-5582(63)90370-5
16. C.H. Johnson, C.C. Trail, A. Galonsky, Thresholds for (p, n) reactions on 26 intermediate weight nuclei. Phys. Rev. B **136**, 1719–1729 (1964). https://doi.org/10.1103/PhysRev.136.B1719
17. R.M. Humes, G.F. Dell, W.D. Ploughe et al., (p, n) Cross Sections at 6.75 MeV. Phys. Rev. **130**, 1522 (1963). https://doi.org/10.1103/PhysRev.130.1522